Laser smoothing of binary gratings and multilevel etched structures in fused silica

Laser smoothing of binary gratings and multilevel etched structures in fused silica

Krystian L. Wlodarczyk,[1,*] Enrique Mendez,[1] Howard J. Baker,[1] Roy McBride,[2] and Denis R. Hall[1]

[1]School of Engineering and Physical Sciences, Heriot-Watt University, Edinburgh EH14 4AS, United Kingdom

[2]PowerPhotonic Ltd, Unit 1, St David's Drive, St David's Business Park, Dalgety Bay, Fife KY11 9PF, United Kingdom

*Corresponding author: klw6@hw.ac.uk

Received 12 October 2009; revised 5 February 2010; accepted 25 February 2010; posted 4 March 2010 (Doc. ID 118058); published 1 April 2010

We describe a promising approach to the processing of micro-optical components, where CO_2 laser irradiation in raster scan is used to generate localized surface melting of binary or multilevel structures on silica, fabricated by conventional reactive-ion etching. The technique is shown to provide well-controlled local smoothing of step features by viscous flow under surface tension forces, relaxing the scale length of etch steps controllably between 1 and 30 μm. Uniform treatment of extended areas is obtained by raster scanning with a power stabilized, Gaussian beam profile in the 0.5 to 1 mm diameter range. For step heights of 1 μm or less, the laser-induced relaxation is symmetric, giving softening of just the upper and lower corners at a threshold power of 4.7 W, extending to symmetric long scale relaxation at 7.9 W, with the upper limit set by the onset of significant vaporization. Some asymmetry of the relaxation is observed for 3 μm high steps. Also, undercut steps or troughs produced by photolithography and etching of a deep 64 level multistep surface are found to have a polarization-dependent distortion after laser smoothing. The laser reflow process may be useful for improving the diffraction efficiency by suppressing high orders in binary diffractive optical elements, or for converting multilevel etched structures in fused silica into smoothed refractive surfaces in, for example, custom microlens arrays.

OCIS codes: 050.1380, 050.1970, 140.3390, 220.4000, 350.3950.

1. Introduction

Etching of transparent substrates, such as fused silica, is a well-established technique for the fabrication of high-performance micro-optical components. Structures can be generated by, for example, standard photolithography processes and reactive-ion etching (RIE) [1,2], or more sophisticated laser-induced backside wet etching [3–5]. Etching techniques allow fabrication of complex, multilevel structures with high surface quality and reproducibility. However, the rapid submicrometer transition between levels associated with simple binary masks causes light scatters into off-axis diffraction orders. Diffraction efficiency of optical components can be improved by a multilevel, multimask etching process; however correct mask alignment of the layers is time consuming and requires submicrometer accuracy. An error at any stage of fabrication may degrade performance of a component, increasing optical losses because more light scatters into higher unwanted diffraction orders. Furthermore, the multimask etching is rather expensive for individual part production. Any technique that reduces the number of masks used in the photolithographic process while maintaining high efficiency of an optical component is highly desirable.

A common technique for generation of quasi-continuous surface profiles in a single-step photolithographic process is gray-scale lithography. This

0003-6935/10/111997-09$15.00/0

technique speeds up the fabrication process of micro-optical components, which is important for mass production. However, a high-quality gray-scale mask can be as expensive as a set of binary masks for the same purpose. Moreover, the process is more sensitive to variations in lithographic materials and process parameters than binary techniques, so the potential cost benefits gained by reducing a number of processing steps can, therefore, be diminished by lower yields [2].

An alternative route to generating a quasi-continuous surface is to place a stepped surface structure into a furnace to induce relaxation of sharp features present in the structure. Often, the initial features are generated by binary masks and etching, but also by embossing/molding methods. A recent example of this technique was the reflow of an array of 10 μm high microcylinders molded on a PSK57 glass substrate [6]. The sample was reheated uniformly to a temperature near the softening point of 600 °C for a fixed time (from 100 to 400 s) to convert the cylinders to microlenses by surface tension driven flow. This process, however, is limited by the initial shape of the etched or molded structure, and it is most easily applied to glasses where the melting point is much less than that of silica. To achieve a similar surface relaxation effect of stepped or binary surface features in fused silica, it is necessary to use a much higher furnace temperature for the reflow effect, at or greater than the 1600 °C softening point. Precise control of the temperature uniformity across a large substrate is needed for a uniform reflow effect, and this is more difficult at this high temperature.

Previously reported work [7–13] has shown that CO_2 laser treatment of glass produces a thin melt layer that flows under the influence of surface tension forces. The laser irradiation causes only a shallow glass layer to melt, because most optical glasses have a high absorption coefficient at the 10.6 μm laser wavelength. CO_2 laser treatment of glass has already been exploited to produce improved laser-damage-resistant surfaces [7], to reduce the surface roughness of bulk optical components [8,9], to repair laser-damage sites [10], and to produce local smoothing of laser-machined micro-optical elements [11–13]. The basic mechanism for surface modification by laser smoothing is the same as that in furnace-based reflow, but the surface temperature is much higher, the surface layer is thin and it has a much lower viscosity, and surface melt flow takes place on a shorter time scale. These result in important differences to the furnace reflow method. The limited melt depth restricts the viscous flow in the melt layer, limiting the smoothing effect to high spatial frequency features on the surface [11]. The diameter of the melt spot produced by the laser also localizes melt flow and is another tool that can be used to control the range of the smoothing effect [10]. The substrate remains below the softening point, preventing the distortion of the geometry of surface features. Consequently, laser smoothing preserves the position accuracy of the initial feature on the surface.

This paper reports the extension of the application range for the CO_2 laser-smoothing technique, by addressing the treatment of the very sharp submicrometer steps associated with the RIE process for the fabrication of binary gratings, diffractive optical elements (DOE), and multistep structures. Here, we investigate laser-induced relaxation of etched steps in the 0.2 to 3 μm height range in silica, for a range of different laser-smoothing conditions. One objective is to show that the process may usefully redistribute and reduce the light scattered into high diffraction orders by simple binary surface structures, requiring effects on a few micrometer scale length, of relevance to DOE applications. A second objective is to find conditions where the staircase in a multilevel structure may be converted to a quasi-continuous surface, requiring relaxation to scale lengths of over 10 μm. This second application can be a new approach to producing arbitrary, quasi-continuous surfaces by combining well-established techniques for the etching of digital optics structures with the a highly controlled laser-smoothing process. Effectively, the smoothing aims to provide a controlled low-pass filter function.

2. Melt Flow by Controlled Heating of Silica

There is an excellent match between CO_2 laser beam characteristics and the properties of silica. The low reflection loss, R, and the high absorption coefficient, α, at the CO_2 laser wavelength [14] results in a well-controlled and rapid surface heating of the irradiated area, generating a thin viscous layer on the surface that flows under the action of surface tension, γ. The low expansion coefficient of silica allows laser surface melting from room temperature with sufficiently low stress on cool down to avoid cracking. The viscosity of the heated (melt) layer decreases exponentially with temperature [15], so that at temperatures above the softening point $T_s \sim 1600$ °C for silica, the material gradually becomes a mobile liquid and ultimately begins to flow. In practice, the upper limit for effective laser smoothing of silica is about 2750 °C. Above this temperature, loss of mass begins to occur by laser-induced vaporization [16]. Therefore, precise control of the peak temperature silica surface is required, in order to control the relaxation of the silica surface to obtain optimum smoothing of the structure while avoiding mass loss.

To achieve better understanding of the dynamics of laser melting for etched steps, it is helpful to consider the relationship between the pressure, P, developed in the interior melt layer, the surface tension, γ, and the principal curvature radius of the surface, R. It has been shown by [17] that there is an inverse dependency of the pressure on the radius of curvature as follows:

$$P = -\frac{\gamma}{R}. \quad (1)$$

This simple view, based on bulk liquid behavior, applies in the case of laser smoothing because the melt depth is typically 20 μm [10], considerably larger than the size of etched features. Equation (1) shows that the highest pressure is generated at the sharpest corners of the etch step, such as the L-shaped step shown in Fig. 1(a). The viscous molten layers immediately adjacent to the sharp corners of the step are moved from this location to sites of lower pressure, thereby causing a reduction in the curvature of the edges of the step, as illustrated in Figs. 1(b) and 1(c).

The rate at which this melt flow occurs depends on the glass viscosity, and, hence, increases rapidly with surface temperature, while the total movement of the surface is controlled by the time the surface is maintained near peak temperature. Thus, in a qualitative sense, one can distinguish stages in the surface relaxation of stepped structures. In Fig. 1(a), with the surface temperature relatively low, the viscous molten layer is pushed from the top corner (Point A) to lower pressure sites creating a small bulge, whereas the bottom corner (Point B) is subjected to the negative pressure that draws glass toward the sharp tip, creating a small hollow, as shown in Fig. 1(b). At this stage, sharp edges are gently rounded without mass transfer down the step. When more intense or subsequent laser irradiation is applied to the now-rounded steps, the viscous forces are acting on a larger area. This reduces the bulges and hollows, and forms a slope between the top and bottom corners [Fig. 1(c)]. At this stage, the molten viscous layer is effectively transferred from the top corner directly to the bottom corner, reducing significantly the slope of the previously near-vertical step. Such strong relaxation leads eventually to complete vanishing of sharp steps, making the structure smooth, as in the reflow process. This schematic view of step smoothing allows us to better understand of the processes that occur with the binary and multilevel structures, described in the following sections.

Laser smoothing necessarily requires transient heating and cooling of the surface to avoid buildup of the substrate temperature. As a surface treatment, it might be expected that a large area pulse of laser energy with low repetition rate would be the preferable route. However, there is a need to limit the surface temperature to a controlled point below the onset of evaporation over the 10 to 100 ms time scale. This requires stable pulse modulation of a high average power CO_2 laser. Conversion of the Gaussian beam of this laser to a flat-top profile by a beam integrator or a flat-top converter optic is extraordinarily difficult, because intensity ripples caused by the long laser wavelength and high spatial coherence preclude the necessary 1% intensity uniformity.

The preferable method is to obtain the required time scale by scanning a stabilized Gaussian beam profile across the surface. A raster scan then provides the area coverage. An advantage is that the smaller melt area acts to limit the unwanted smoothing of low spatial frequency components of the test piece. In the following sections, a continuous-wave RF excited CO_2 laser is used, with a closed-loop beam power controller based on a reference power meter and an acousto-optic modulator. This provides a stability of 1% at 10 W and a power regulation resolution of 0.1%. A motorized XY table moves samples under the fixed beam. The sample is in contact with an aluminum plate to act as a heat sink.

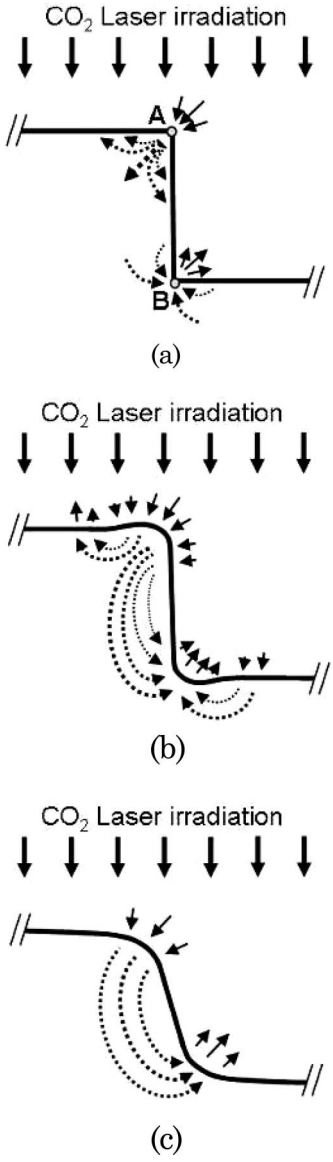

Fig. 1. Surface relaxation of the etched structure by CO_2 laser irradiation. Solid arrows indicate the significant pressure acting on the molten edges, whereas dotted arrows indicate the liquid flow.

3. Smoothing of a Binary Optic Surface by Laser Line Scan

In an initial set of experiments designed to calibrate the CO_2 laser-smoothing process, a single linear scan laser treatment was performed on a simple periodic binary structure in fused silica. The etched steps of the grating were 1 μm high and their spatial period

was 22.6 μm, as illustrated in Fig. 2(a). The fundamental mode Gaussian beam with diameter of $\sim$1 μm was moved perpendicular to the etched grooves on the silica surface with a feed rate of 5 mm/s. From previous work [11], we know that such a laser beam diameter produces up to a 200 μm wide melt track, d_m, which is much larger than features of the treated object, giving effective smoothing while limiting the laser power needed. For these irradiation conditions, the relaxation of the sharp edges of the sample was investigated for increasing numbers of overlapped laser scans, N, and different laser power levels, up to the point where mass loss first appears due to evaporation.

Figure 2(b) gives an initial view of the smoothing process using ten fully overlapping line scans. The onset of a visible smoothing effect occurs at laser power of 7.35 W and this can be seen as an $\sim$120 μm wide modification in the groove appearance. This corresponds to the width over which the surface temperature rises above $\sim$2000 °C. As the laser power is increased to 7.85 W, the depth and width of the molten layer increases and the viscosity reduces

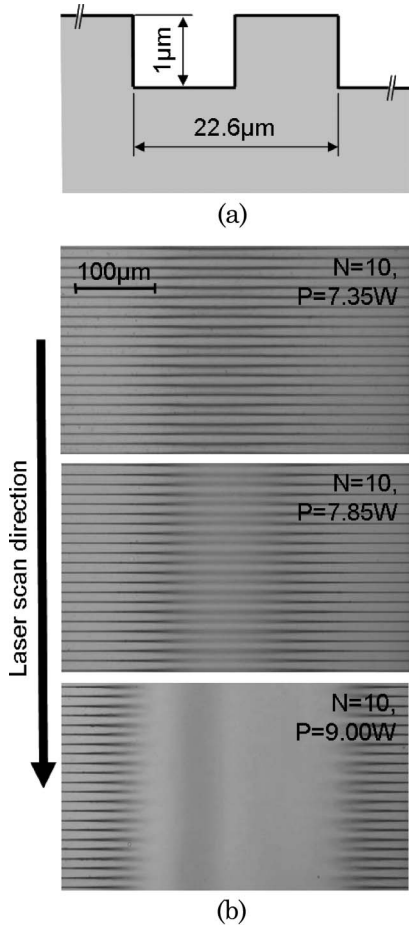

Fig. 2. (a) Illustration of the binary grating with spatial period of 22.6 μm and step height of 1 μm. (b) Micrographs of the structure after laser treatment with $N = 10$ unidirectional scans in the direction shown, for laser power of 7.35 W, 7.85 W, and 9.00 W, respectively.

and the blurred line becomes wider, with the horizontal lines representing step edges more difficult to distinguish. At 9.0 W, the high center-line temperature on the surface causes noticeable mass loss by thermal evaporation over a 100 μm width, in addition to removing grating modulation over a 300 μm width by the smoothing process. Figure 2(b) illustrates that the laser-smoothing process is characterized by a limited range of laser powers between the onset of the smoothing effect and removal of material by evaporation. To exploit the process, it is necessary to have a power-controlled laser source, as described in Section 2, with a stable beam shape and diameter at the surface.

Since the optical micrographs in Fig. 2(b) do not directly show the extent of the relaxation of etched edges, profiles of the sample were obtained using a Dektak profilometer. As a means to quantify the step relaxation, we introduce a parameter, the relaxation distance, which is defined as the distance between two points where the edge profile reaches 10% and 90% of the original step height, labeled as RD in Fig. 3. The set of edge profiles obtained at the constant laser power and at varied numbers of laser scans is shown in Fig. 3. A single scan at laser power of 7.35 W is observed to relax steps to a RD $\sim$ 2 μm with no mass loss. Increasing the number of laser scans builds up the smoothing effect, due to the longer total time at which the surface is above the temperature for viscous melt flow. This enlarges the relaxation distance up to $\sim$4.5 μm (for $N = 10$) with slight step height degradation. The maximum measurable value of RD is limited by the width of a single step in a binary grating. In all the cases in Fig. 3, the smoothing effect appears symmetric for the 1 μm step height, consistent with a linear viscous flow and uniform surface temperature.

4. Raster Scan Area Treatment of Binary Gratings

From a practical point of view, a raster scan area treatment of etched structures is more desirable

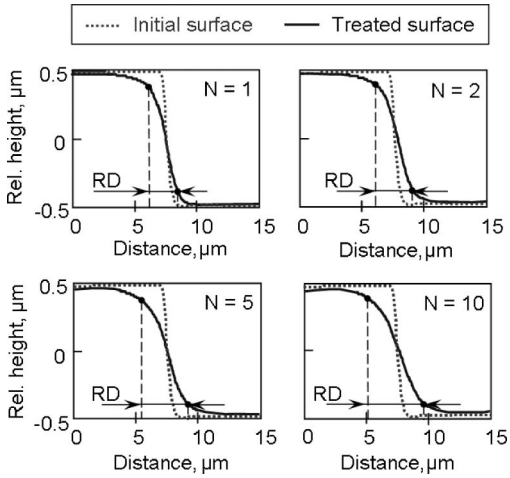

Fig. 3. Evolution of the step profile of the binary grating as a function of laser line scans, N, with fixed laser power, $P = 7.35$ W. The diameter of the laser beam was $\sim$1 mm.

because the moving laser beam covers a larger area of the etched structure, producing a uniform smoothing effect. In this experiment, the raster pitch is much smaller than the diameter of the melt pool so that successive laser scans partially overlap each other. This means that the smoothing effect is stronger than a single laser scan because of a larger accumulated treatment time. It can be comparable to the treatment time in the multipass scan of a single line from Section 3, for equal laser-smoothing conditions, i.e., when laser beam size and laser power used for both cases are the same. In this situation, the equivalent number of overlapping scans, N, can be estimated by

$$N \approx \frac{\pi \cdot d_m}{4 \cdot \Delta x}, \tag{2}$$

on condition that $d_m \geq 10 \cdot \Delta x$, where d_m is the melt spot diameter and Δx is the raster pitch used.

Raster scan area treatment was performed for binary grating samples with steps of height equal to 0.8 and 3 μm, with a 22.6 μm period. Each sample was treated with laser powers in the range from 4.45 to 8.95 W. The laser spot, with a Gaussian beam diameter of ~550 μm in this case, was scanned normal to the etched edges with a feed rate of 5 mm/s and the raster pitch was $\Delta x = 10\,\mu$m. As reported in [11], this laser spot size generates ~100 μm diameter melt zones. Figure 4 shows single line traces taken by atomic force microscope (AFM) for both 0.8 and 3 μm depth binary gratings for laser powers of 5.7 W and above. For the 0.8 μm binary grating [Fig. 4(a)] treated with laser powers of 5.7 and 6.2 W, we observe bulges and hollows near the step corners, corresponding to the smoothing condition illustrated by Fig. 1(b). For the 6.7 W laser power, the bulges and hollows disappear and the amplitude of the grating begins to reduce. Here, the higher surface temperature and, hence, lower silica viscosity are sufficient for melt flow over the full period of the grating. Further increase of laser power to 7.7 W almost completely relaxes the square grating profile, reducing significantly the amplitude of the grating and producing a near-sinusoidal profile.

The profiles in Fig. 4(a) for the 0.8 μm amplitude grating show good symmetry of the smoothing effect between the top and bottom half cycles. However, the surface profiles for the 3 μm amplitude grating in Fig. 4(b) treated at the same laser powers show clear asymmetry in smoothing of the top and bottom corners, especially noticeable for samples treated with laser powers from 5.7 to 6.7 W. There is a tendency for the lower corners to be undersmoothed. The effect is modified to some extent by the inability of the AFM profilometer stylus to follow the actual shape of deep corners, as shown by the surface profile with 5.7 W treatment. The asymmetry remains clearly defined at laser powers ≥6.2 W, where the grating is relaxed toward the weak sinusoidal shape. We consider that relaxation asymmetry of s 3 μm binary grating may be associated with an absorption depth comparable

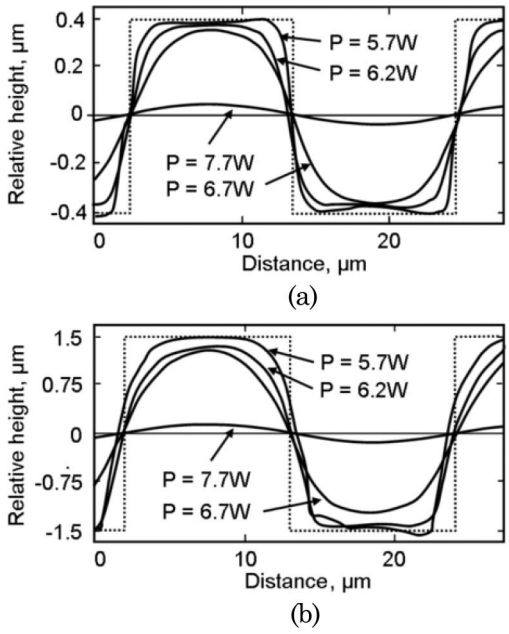

Fig. 4. AFM surface profile of laser-treated binary samples with (a) 0.8 μm initial step height and (b) 3 μm initial step height. Dotted line indicates ideal shape of a binary grating before laser smoothing. The diameter of the laser beam used was ~550 μm.

to the grating height, combined with the use of a laser whose wavelength is larger than the features being smoothed, and thus producing a nonuniform heating effect. McLachlan and Meyer reported that the absorption depth, β, of fused silica at the CO_2 (10.59 μm) laser wavelength decreases significantly with temperature, from 34 μm at room temperature to ~4.2 μm at 1800 °C [18]. The extrapolation of the absorption depth for 2500 °C, where the strong relaxation of steps is obtained, gives $\beta \sim 3\,\mu$m, which is comparable to the step size of binary gratings. Such small absorption depth may cause a nonuniform heating effect on the surface so that the upper part of the step is hotter than the bottom section. The relaxation asymmetry may also be amplified by the fact that the extent of features in the structure (the step height and the step repetition) is comparable with the wavelength of the laser, making a nonuniform heat distribution along the step profile. The interaction of light with subwavelength features has been described, e.g., in [19,20]; however, those publications do not give us a simple answer for this particular problem.

Surface profiles were measured by both an AFM and a Dektak profilometer; however, neither instrument responded accurately when the walls of the etched steps were near vertical. This meant that the weak smoothing effect, as schematically shown in Fig. 1(a), cannot be measured by the stylus-based instruments. Since an objective is to fully characterize the small-scale relaxation and determine the threshold for the process, an optical method was used to observe the effect of surface melting. A He–Ne laser beam transmitted normal to the substrate

surface was split by the phase grating into a large number of diffraction orders that were individually measured by a movable photodetector. Figure 5 shows the evolution of the measured diffraction spectrum of positive orders for the grating step height of $0.8\,\mu$m. The untreated initial surface acts as a square-wave phase grating with a phase shift of $\sim 1.3\pi$ at 633 nm, and the intensity of the even orders is found to be low, suppressed, as expected, by the grating symmetry and the sharpness of the steps. We observe the onset of the smoothing effect at a CO_2 laser power of 4.7 W, where laser irradiation starts flow just at the sharp corners of the periodic structure as an increase in the low initial intensity of the even diffraction orders.

At the higher smoothing powers, where satisfactory stylus-based profiles can be obtained, as in Fig. 4(a), the odd and even diffraction equalize, forming a sloping line, as shown in Fig. 5 for laser power of 5.7 W. At 7.7 W, smoothing is to the point where only the two lowest diffractive orders are significant, consistent with the grating being converted to a sinusoidal weak phase grating. The sequence in Fig. 5, with the exception of changes just at the 4.7 W threshold, has been shown to be consistent with diffraction integral calculations carried out for a model square-wave grating, smoothed by applying a Gaussian low-pass filter of increasing bandwidth. This is evidence that the effect of step smoothing for small amplitude features may be regarded as application of a low-pass filter of controlled bandwidth, similar to that reported previously in [11]. Observation of the diffraction pattern from a grating test pattern may be a useful rapid diagnostic tool for setup of the laser-smoothing conditions in applications on more complex binary DOEs, or multistep surfaces, as in Section 5.

Comparison of the profiles of 0.8 and $3\,\mu$m binary gratings for laser powers at which significant step height reduction was found ($P > 7.2$ W) shows that the amplitude of the sinusoid is proportional to the initial step height of the binary grating used. However, the additional He–Ne laser diffraction analysis has shown that a near-sinusoidal shape for a $3\,\mu$m grating is more difficult to obtain and requires using higher smoothing power, because of the relaxation asymmetry discussed earlier.

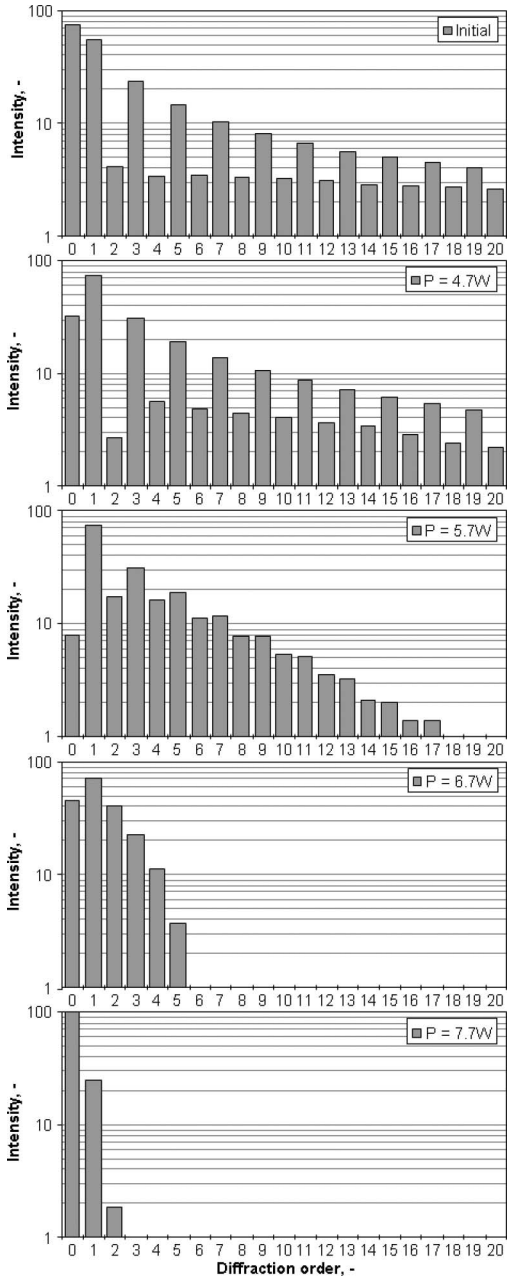

Fig. 5. Light scatter distribution versus diffraction order at different raster scan laser treatment conditions of the binary grating with step height of $0.8\,\mu$m.

5. Laser Smoothing of Multistep Optics

Since CO_2 laser smoothing of binary gratings has shown controllable relaxation of single-level features, we want to extend this process to laser smoothing of multilevel etched elements. We believe that such an approach may be a useful alternative to the glass reflow process in the case where silica glass is used to fabricate refractive micro-optical components, such as a single microlens or microlens arrays [6]. Additionally, the ability to "dial up" a required bandwidth of a low-pass filter may be of value to improve the diffraction efficiency of multistep blazed gratings made by the multilevel etching process. Previously, it has been shown mathematically that an optimal Gaussian filter bandwidth can be defined for smoothing of the triangular profile of stepped blazed grating [21].

To demonstrate the usefulness of laser relaxation of multistep structures, we applied smoothing to two identical silica samples with 64 steps that had been produced by a multimask RIE process. Six different masks were used in sequence to fabricate both samples. The height of each step was 200 nm, giving a total structure height of $12.8\,\mu$m. The horizontal distance between steps was in the range from 50 to $1500\,\mu$m at various positions across the sample, giving the opportunity to study long-range relaxation of an isolated step. However, microscope analysis of

these samples also showed some of the transitions in the multistep structures had undercut steps or deep grooves, created presumably by mask misalignment during the photolithographic process, combined with large overall etch depth. Such a diversity of features on the etched surface makes this sample very valuable from the research point of view, because it includes all extreme etching cases on one piece.

Since raster area treatment has produced a uniform smoothing effect for a specific case of a binary grating in Section 4, we have also applied this mode to the multistep sample. The laser-smoothing conditions were similar to those for laser treatment of binary optics, with the exception that the laser beam size used was increased back to ~1mm diameter.

One of the 64-step samples was smoothed with laser power of 7.6 W and the second with 7.9 W, with the objective of investigating larger relaxation distances than possible with the 22.6 μm period grating. The surface profile of relaxed features was measured by a Dektak profilometer and compared with the initial surface shape. In addition, an optical microscope was used to examine the overall structure. The microscope image of the sample before laser smoothing is shown in Fig. 6(a). There are visible, sharp zigzag steps that fall from top to bottom, crossing an ~8 μm wide groove, marked as the horizontal center line on the micrograph. This groove, located between the 31st and 32nd levels, was created presumably by a mask registration error in the second photolithographic step, so its depth could be up to ~6.4 μm. After laser smoothing with laser power of 7.6 W, the zigzag steps seem to be softened, whereas the groove appears wider, as shown in Fig. 6(b).

To investigate the surface relaxation of staircase steps, the marked regions in Fig. 6 were scanned using the Dektak profilometer. The radius of the profilometer stylus used was 12.5 μm, giving 2.2 μm broadening of the 200 nm high steps. Figure 7 shows the surface profile of the staircase steps, marked as the A and A′ areas in Fig. 6. The initial surface has an ~9 μm edge width and so is defined by the etching process, rather than the stylus limit. Laser smoothing of such low steps relaxes them symmetrically, with a step profile close to the error function shape expected for a Gaussian low-pass filter effect. Relaxation distances of 20 μm at 7.6 W treatment power and 30 μm at 7.9 W were determined from Fig. 7. With allowance for the initial step width, the relaxation effect from laser smoothing is 18 μm at 7.6 W and 28 μm at 7.9 W. In this part of the sample area, with small step height and no undercut edges, laser smoothing is the same for edges oriented at all directions relative to the scan direction, and for the corners of the zigzag pattern, thus showing no dependence on the incident laser polarization direction.

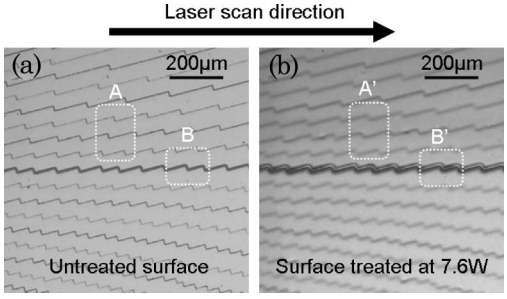

Fig. 6. Microscope image of (a) the untreated multilevel etched structure, with visible zigzag steps and a groove in the middle, and (b) the same sample after laser treatment at laser power of 7.6 W.

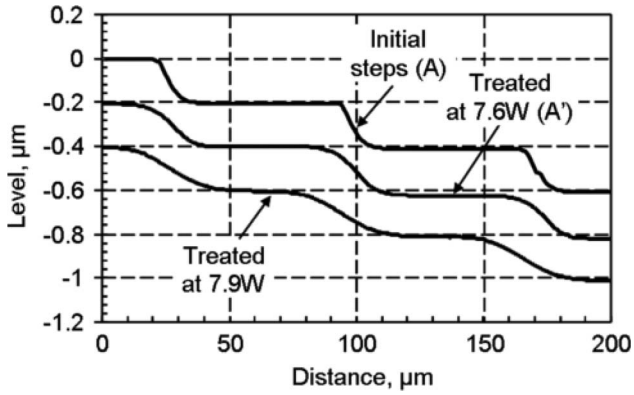

Fig. 7. Laser smoothing effect of "normal etched" steps, marked as the A area in Fig. 6(a), at different laser powers. Each profile is offset by 0.2 μm.

The smoothing effect on the deep central groove discussed previously has been separately investigated in areas B and B′ of Fig. 6. Scanning of this deep feature using the Dektak profilometer gives the initial groove trace in Fig. 8 that is 12 μm wide and ~0.7 μm deep. This trace is purely limited by the stylus response, because the size of the tip used is larger than the initial undercut width. After laser treatment, the groove trace becomes wider and deeper, especially at laser power of 7.9 W, where it is 36 μm wide and ~2.2 μm deep. Although the increase in width at the surface is correctly indicated, the stylus does not reach the bottom of the groove, so the depth may be underestimated. Our estimates of the initial groove area was 6.4 μm deep and 8 μm wide before laser smoothing, and the Dektak trace appears to have a larger area for the 7.9 W laser

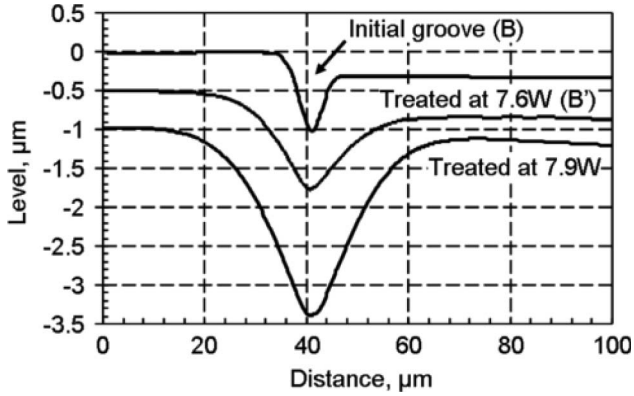

Fig. 8. Laser smoothing effect of the misregistered region, marked as the B area in Fig. 6(a), at different laser power. Each profile is offset by 0.5 μm.

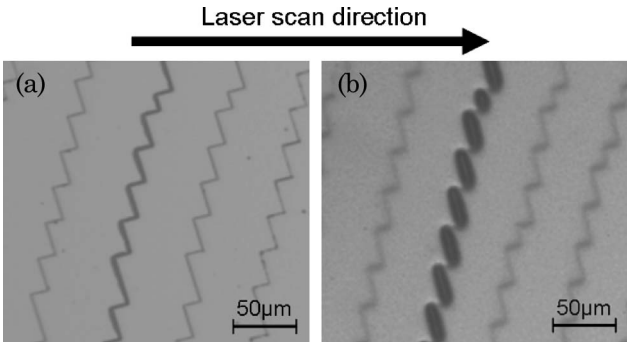

Fig. 9. Misregistered etch steps oriented perpendicular to the scan direction (a) before and (b) after laser treatment with laser power of 7.6 W.

power. This effect may be caused by the subwavelength interaction of light with the initial groove feature, as is comparable in size to the wavelength of the laser, producing a localized hot spot [20].

For deep groove or undercut features, we also observed that the direction of the laser scan motion matters. As shown in Fig. 9, misregistered features orientated normal to the direction of the moving laser beam became longitudinal pits following laser treatment, whereas a molten layer of glass filled in the grooves parallel to the laser scan direction. This effect is explained by the polarization dependency between the submicrometer features and the laser beam used, reported by [19]. The pattern of longitudinal pits may also be associated with the capillarity during the laser-smoothing process when glass becomes liquid and flows under surface tension effect. This effect was previously observed in laser-smoothed diamond scribe lines in fused silica [10].

6. Conclusion

We have shown that CO_2 laser irradiation provides well-controlled relaxation of the sharp edges in etched structures in silica. The raster scan technique using a moderate laser power in the 10 W region, but with high-accuracy power control, produces excellent uniformity of treatment for incident laser spots of a diameter in the 0.5 to 1 mm range. Typical scans at 5 mm/s with 10 μm raster steps treat the surface at a rate of only 1.8 cm^2/h, but that is sufficient for applications in custom and prototype micro-optics. Scaling of the process speed may be possible by proportional increases in laser power, spot area, and scan pattern, with a factor of 4 in speed expected not to affect the principle features of the process. Further scaling may use multiple spots in parallel, as CO_2 lasers are low-cost sources, and this may bridge across to treatments for smaller diameter wafer production. At higher speeds, substrate cooling may need improvement.

By tests on a variety of RIE etched silica components, we have shown that laser power control can adjust the relaxation distance from submicrometer at 4.7 W to 30 μm at 7.9 W with the raster scanning producing uniform treatment. The steps are relaxed symmetrically over this scale size for step heights of up to 1 μm, without laser polarization dependence, and with increasing asymmetry of smoothing for larger step heights. A particular limitation of this process is when undercut features are present from imperfections in multistep etched components. The laser treatment cannot smooth them out and produces a polarization-dependent, nonlinear distortion in the structure, enhancing the appearance of defects. This laser-smoothing technique is promising as part of the fabrication of reduced light scatter micro-optical components using binary or multilevel etched structures as a precursor.

The authors acknowledge M. Taghizadeh and N. Ross from the Diffractive Optics Group at Heriot-Watt University for the fabrication of etched structures used in the experiments. This work has been supported by the Engineering and Physical Sciences Research Council (EPSRC, UK), the Heriot-Watt Innovative Manufacturing Research Centre (IMRC, UK), and the Edinburgh Research Partnership (ERP, UK).

References

1. S. Sinzinger and J. Jahns, "Fabrication of diffractive optics," in *Microoptics* (Wiley-VCH, 1999), pp. 129–179.
2. R. G. Driggers, "Diffractive optics fabrication," in *Encyclopedia of Optical Engineering: Vol. 1* (Marcel Dekker, 2003), pp. 374–388.
3. K. Zimmer and R. Bohme, "Precise etching of fused silica for refractive and diffractive micro-optical applications," Opt. Lasers Eng. **43**, 1349–1360 (2005).
4. C. Vass, K. Osvay, M. Csete, and B. Hopp, "Fabrication of 550 nm gratings in fused silica by laser induced backside wet etching technique," Appl. Surf. Sci. **253**, 8059–8063 (2007).
5. G. Kopitkovas, T. Lippert, J. Venturini, C. David, and A. Wokaun, "Laser induced backside wet etching: mechanisms and fabrication of micro-optical elements," J. Phys. Conf. Ser. **59**, 526–532 (2007).
6. Y. Chen, A. Y. Yi, D. Yao, F. Klocke, and G. Pongs, "A reflow process for glass microlens array fabrication by use of precision compression molding," J. Micromech. Microeng. **18**, 055022 (2008).
7. P. A. Temple, W. H. Lowdermilk, and D. Milam, "Carbon dioxide laser polishing of fused silica surfaces for increased laser-damage resistance at 1064 nm," Appl. Opt. **21**, 3249–3255 (1982).
8. F. Laguarta, N. Lupon, and J. Armengol, "Optical glass polishing by controlled laser surface-heat treatment," Appl. Opt. **33**, 6508–6512 (1994).
9. F. Vega, N. Lupon, J. A. Cebrian, and F. Laguarta, "Laser application for optical glass polishing," Opt. Eng. **37**, 272–279 (1998).
10. E. Mendez, K. M. Nowak, H. J. Baker, F. J. Villarreal, and D. R. Hall, "Localized CO_2 laser damage repair of fused silica optics," Appl. Opt. **45**, 5358–5367 (2006).
11. M. Nowak, H. J. Baker, and D. R. Hall, "Efficient laser polishing of silica micro-optic components," Appl. Opt. **45**, 162–171 (2006).
12. J. F. Monjardin, K. M. Nowak, H. J. Baker, and D. R. Hall, "Correction of beam errors in high power laser diode bars and stacks," Opt. Express **14**, 8178–8183 (2006).
13. N. Trela, H. J. Baker, J. J. Wendland, and D. R. Hall, "Dual-axis beam correction for an array of single-mode diode laser

emitters using a laser-written custom phase-plate," Opt. Express **17**, 23576–23581 (2009).
14. H. R. Philipp, "Silicon dioxide SiO_2 (glass)," in *Handbook of Optical Constants of Solids*, E. D. Palik, ed. (Academic, 1985), pp. 749–763.
15. R. H. Doremaus, "Viscosity of silica," J. Appl. Phys. **92**, 7619–7629 (2002).
16. G. A. J. Markillie, H. J. Baker, F. J. Villarreal, and D. R. Hall, "Effect of vaporization and melt ejection on laser machining of silica glass micro-optical components," Appl. Opt. **41**, 5660–5667 (2002).
17. E. Guyon, J. Hulin, L. Petit, and C. Mitescu, "The physics of fluids," in *Physical Hydrodynamics* (Oxford U. Press, 2001), pp. 31–40.
18. A. D. McLachlan and F. P. Meyer, "Temperature dependence of the extinction coefficient of fused silica for CO_2 laser wavelengths," Appl. Opt. **26**, 1728–1731 (1987).
19. M. G. Moharam, E. B. Grann, and D. A. Pommet, "Formulation for stable and efficient implementation of the rigorous coupled-wave analysis of binary gratings," J. Opt. Soc. Am. A **12**, 1068–1076 (1995).
20. M. Mansuripur, A. R. Zakharian, and J. V. Moloney, "Interaction of light with subwavelength structures," Opt. Photonics News **14**(3), 56–61 (2003).
21. M. Kuittinen, H. P. Herzig, and P. Ehbets, "Improvements in diffraction efficiency of gratings and microlenses with continuous relief surfaces," Opt. Commun. **120**, pp. 230–234 (1995).